Scientific Contributions Oil & Gas, Vol. 49. No. 1, March: 359 - 373

SCIENTIFIC CONTRIBUTIONS OIL AND GAS

Testing Center for Oil and Gas
LEMIGAS

Journal Homepage:http://journal.lemigas.esdm.go.id
ISSN: 2089-3361, e-ISSN: 2541-0520

Caprock Integrity Assessment from Core-Based Formation Analysis and Laboratory Workflow: A Case Study of The Asri Basin Caprock

Aris Buntoro[1], Teddy Eka Putra[4], Dedi Kristanto[1], Boni Swadesi[1], Zulhemi Amir[2], Allen Haryanto Lukmana[1], Dimas Suryo Wicaksono[1], and Mohammad Nurcholis[3]

[1]Department of Petroleum Engineering, Universitas Pembangunan Nasional "Veteran" Yogyakarta
Padjadjaran Street (North Ring Road), Condongcatur, Depok, Sleman, Yogyakarta, 55283, Indonesia.

[2]Department of Chemical Engineering,Faculty of Engineering, University of Malaya
50603 Kuala Lumpur, Malaysia.

[3]Department of Soil Science,Faculty of Agriculture,Universitas Pembangunan Nasional "Veteran" Yogyakarta
Padjadjaran Street (North Ring Road), Condongcatur, Depok, Sleman, Yogyakarta, 55283, Indonesia.

[4]Upstream Innovation at PT Pertamina Hulu Energi-Subholding Upstream
[4]PHE Tower, 22nd Floor, TB Simatupang Street Kav. 99 Kebagusan, Pasar Minggu, South Jakarta, Indonesia.

Corresponding author: Aris Buntoro (arisbuntoro@upnyk.ac.id)

Manuscript received: February 03th, 2026; Revised: February 26th, 2026
Approved: February 27th, 2026; Available online: March 23th, 2026; Published: March 23th, 2026.

ABSTRACT - Caprock integrity is a critical factor in ensuring the long-term safety of CO_2 geological storage, enhanced oil recovery (EOR), and wellbore stability. This study investigates the sealing performance of shale- and carbonate-rich caprock intervals from the Asri Basin, with specific focus on the Baturaja and Gita Formations. This study introduces a CT-guided integrated laboratory workflow for caprock integrity assessment, which simultaneously links petrophysical sealing capacity, mineralogical controls, and geomechanical strength within a unified experimental framework, a workflow rarely applied in Southeast Asian basins. Whole-core sections from Well ASR-1 were screened using computed tomography (CT) imaging to identify fractures and heterogeneity prior to plug extraction. Laboratory methods included porosity and permeability determination under variable confining stresses, mercury injection capillary pressure (MICP) analysis to evaluate sealing capacity, mineralogical characterization by X-ray diffraction (XRD), scanning electron microscopy (SEM–EDS), petrography, and mechanical testing (UCS, triaxial, and Brazilian tensile tests). The results demonstrate significant depth-dependent variability: The Baturaja Formation exhibited heterogeneous sealing capacity, with entry pressures ranging from 217 to 1,197 psi, while the Gita Formation consistently displayed strong sealing, with maximum Pc_entry of 2,844 psi and pore systems dominated by <0.1 μm throats. Mechanical tests confirmed adequate strength and the preservation of low permeability under confining stress, with clay content and carbonate cementation identified as primary controls on integrity. The integrated workflow enables a process-based interpretation

of lithology-controlled sealing mechanisms, improving the robustness of site selection and risk assessment for CO_2 storage in the Asri Basin and similar carbonate and mudstone systems.

Keywords: caprock integrity, core analysis, formation stratigraphy, petrophysics, rock mechanics.

How to cite this article:

Aris Buntoro, Teddy Eka Putra, Dedi Kristanto, Boni Swadesi, Zulhemi Amir, Allen Haryanto Lukmana, Dimas Suryo Wicaksono, and Mohammad Nurcholis, 2026, Caprock Integrity Assessment from Core-Based Formation Analysis and Laboratory Workflow: A Case Study of The Asri Basin Caprock, Scientific Contributions Oil and Gas, 49 (1) pp. 359-373. DOI org/10.29017/scog.v49i1.2021.

INTRODUCTION

The integrity of the caprock determines the long -term security of subsurface energy operations, particularly carbon capture and storage (CCS), enhanced oil recovery (EOR), and wellbore safety (Ajayi et al., 2019; Busch et al., 2008). Caprock failure can lead to uncontrolled fluid migration, compromising storage capacity and posing environmental and operational hazards (Miocic et al., 2019; Skerbisch 2025). Although numerous studies have investigated reservoir performance, comparatively fewer have established systematic approaches for evaluating the overlying caprock, despite its role as the ultimate barrier for CO_2 containment (Lohr & Hackley 2018; Paulsen 2022). Previous research has emphasized the relevance of petrophysical sealing capacity (capillary entry pressure, stress-sensitive permeability), mineralogical composition (clay fabrics and carbonate cementation), and rock mechanics (strength parameters) in determining caprock integrity (Boulin et al., 2013; Farokhpoor et al., 2013; Hansen 2020; Lin 2022).

Recent advances have introduced workflows that integrate multi-scale imaging and laboratory testing to address heterogeneity in caprock lithologies (Bera et al., 2025; Chiquet et al., 2007; Kadyrov et al., 2024). However, significant gaps remain. First, the variability of sealing properties within a single stratigraphic interval is often underrepresented in regional assessments (Fisher et al., 2001; Miocic et al., 2019). Second, the coupling of mineralogical controls with mechanical strength has not been systematically addressed in case studies from Southeast Asian basins, including Indonesia (Skerbisch 2025). Third, laboratory workflows often isolate petrophysical, geochemical, and mechanical analyses rather than integrating them within a single experimental program (Ali 2021; Ao et al., 2017; Choi et al., 2021; Klewiah et al., 2020; Zou 2018).

This study addresses these gaps through a core-based workflow applied to the Asri Basin. By combining CT-guided core screening, petrophysical characterization, mineralogical analyses, and rock mechanics testing, a robust assessment of caprock integrity is generated (Boulin et al., 2013; Lohr & Hackley 2018; Nugraha et al., 2024). The focus is on shale- and carbonate-rich intervals of the Baturaja and Gita Formations in Well ASR-1, which represent the principal sealing units in this basin. The findings are directly applicable to CCS site selection, EOR planning, and wellbore stability management, offering new insights into lithology-dependent variability of sealing capacity in Indonesian caprock systems (Busch et al., 2008; Destiana et al., 2025; Farokhpoor et al., 2013; Paulsen 2022).

The Asri Basin, located offshore southeast Sumatra, Indonesia, is a prolific petroleum province with well-documented carbonate and siliciclastic successions.

Hydrocarbon accumulations are primarily trapped within structural closures of the Talang Akar and Baturaja Formations, sealed by regionally extensive mudstone and carbonate-rich intervals.

The stratigraphic framework relevant to this study includes the Baturaja and Gita Formations, which constitute the principal caprock units above reservoir intervals.

The Baturaja Formation is composed predominantly of shallow-marine carbonates interbedded with argillaceous layers, forming a mixed carbonate–mudstone sequence that locally acts as a seal. Its fine-grained carbonate matrix with subordinate clay content provides moderate to strong sealing capacity. However, heterogeneities such as interparticle porosity and diagenetic dissolution features may locally reduce its sealing integrity.

Overlying the Baturaja, the Gita Formation comprises calcareous claystone, mudstone, and marl, deposited in a more distal marine environment. The higher clay fraction and finer pore structure of the Gita Formation make it a more effective regional caprock. Previous regional mapping has identified the Gita as the primary seal in several CO_2 storage and hydrocarbon fields within the Asri Basin.

Although caprock integrity evaluation is commonly performed in subsurface projects, this study advances beyond routine practice by proposing a CT-guided, fully integrated core-based workflow that systematically couples petrophysical sealing capacity, mineralogical controls, and geomechanical strength within a single experimental framework. While significant progress has been made in evaluating petrophysical properties such as capillary entry pressure (Pc_entry) and permeability, there remains a critical gap in understanding how multifaceted factors, including mineralogy, pore structure, and mechanical strength, interact to influence sealing performance.

This integrated approach enables a process-based interpretation of lithology-dependent sealing mechanisms, rather than a partial or discipline-specific evaluation. The Baturaja and Gita formations provide an appropriate laboratory to demonstrate how integrated multi-scale laboratory data can improve of caprock qualification for CCS applications in Indonesian basin settings.

METHODOLOGY

Whole-core samples from Well ASR-1 were collected at selected intervals across the Baturaja and Gita Formations, which represent caprock intervals overlying the reservoir. Each core interval was documented in terms of measured depth (ft MD) and lithostratigraphic unit, as summarized in Table 1. Upon arrival at the laboratory, the cores were preserved in sealed wrapping, stored at room temperature for at least twenty-four hours, and then conditioned prior to preparation. Representative plugs were subsequently extracted based on computed tomography (CT) imaging to ensure minimal structural damage and to capture lithological heterogeneity.

Table 1. Core intervals and stratigraphic assignment (Well ASR-1)

Depth (ft-MD)	Formation	Remark
3456	Baturaja	Caprock Interval
3562	Baturaja	Caprock Interval
3665	Gita	Caprock Interval
3701	Gita	Caprock Interval
3710	Gita	Caprock Interval
3744	Gita	Caprock Interval

All core sections underwent CT scanning to identify internal features such as natural fractures, mud invasion, and heterogeneities. The results of these scans guided both the orientation and the location of plug extraction (Bera et al., 2025; Kadyrov et al., 2024). Similar workflows have been adopted in recent multiscale caprock investigations, where CT and imaging methods were used to detect microfractures and guide representative subsampling prior to destructive testing (Bera et al., 2025; Busch et al., 2008; Kadyrov et al., 2024).

Cylindrical plugs with a diameter of 25.4 mm and a length between 1.5 to 2 times the diameter were prepared in both horizontal (parallel to bedding) and vertical (perpendicular to bedding) orientations. Horizontal plugs were primarily used for petrophysical characterization, while vertical plugs were reserved for rock mechanics testing.

Additional sub-trims were obtained for scanning electron microscopy (SEM), X-ray diffraction (XRD), and petrographic thin-section analysis. All plugs were cleaned using Soxhlet extraction with toluene/IPA and subsequently dried in a vacuum oven at 60–80 °C until mass stabilization (<0.1% per 24 h) was achieved.

Petrophysical characterization included the measurement of porosity using helium pycnometry, while gas permeability was determined under steady-state flow at multiple confining pressures to evaluate stress sensitivity, with Klinkenberg correction applied where necessary (Bourbiaux 2007; Liang 2022; Lin 2022). Mercury Injection Capillary Pressure (MICP) tests were also performed to determine pore-throat size distribution, threshold and entry pressures, and sealing capacity (Boulin et al. 2013; Hansen 2020; Lohr and Hackley 2018). These measurements are consistent with previous caprock studies that highlight the importance of capillary entry pressure and stress-sensitive permeability in evaluating sealing capacity for CO_2 storage and saline aquifers (Miocic et al., 2019; Paulsen 2022; Skerbisch 2025).

Mineralogical and microstructural analyses were conducted by combining XRD, SEM–EDS, and petrography. XRD was carried out on both bulk and clay fractions to quantify mineral composition using Rietveld refinement for phase quantification. SEM coupled with energy-dispersive X-ray spectroscopy (EDS) was employed to examine pore morphology, clay distribution, and cementation fabrics, while petrographic thin sections were analyzed under polarized light microscopy to evaluate textures, grain size, and diagenetic features (Mouzakis et al. 2016; Olabode and Radonjic 2014). Similar combined mineralogical–microstructural workflows have been applied in caprock integrity studies to establish the role of clay fabrics and carbonate cementation in governing sealing behavior (Ao et al., 2017; Busch et al., 2008; Choi et al., 2021).

Rock mechanical testing was conducted on vertically oriented plugs (Purba et al. 2017). Unconfined compressive strength (UCS) tests followed ASTM D7012, with static Young's modulus and Poisson's ratio derived from stress–strain curves. Triaxial compression tests were performed at confining pressures between 5 and 30 MPa to establish Mohr–Coulomb strength parameters (cohesion and friction angle). In addition, indirect tensile strength was measured using the Brazilian test in accordance with ASTM D3967, providing supplementary data for defining the failure envelope of the caprock material. The integration of petrophysical and mechanical datasets for caprock stability assessment has also been emphasized in recent case studies, where changes in porosity and permeability under CO_2-rich conditions were directly linked to weakening or alteration of seal properties (Al-Yaseri et al., 2023; Choi et al., 2021; Zou 2018). The overall workflow in Figure 1 includes CT scanning, plug extraction, cleaning and drying, petrophysical

Table 2. Laboratory workflow and corresponding measurements

Step	Test/preparation	Purpose	Standard/reference
1	CT scanning	Identify fractures and heterogeneity	ASTM D8144
2	Plug extraction (H/V)	Specimen preparation	ISRM/ASTM
3	Soxhlet cleaning + drying	Remove fluids, stabilize weight	API RP 40
4	Helium pycnometry	Porosity, grain volume	ASTM D4404
5	Steady-state gas permeameter	Permeability (stress sensitivity)	API RP 40
6	Mercury Injection (MICP)	Pore-throat distribution, sealing capacity	ASTM D4404
7	XRD (bulk & clay)	Mineralogical composition	Rietveld refinement
8	SEM–EDS	Pore morphology, clay distribution	ISO 22309
9	Thin-section petrography	Texture, diagenesis	Standard methods
10	UCS test	Compressive strength, E, ν	ASTM D7012
11	Triaxial compression	Cohesion, friction angle	ISRM methods
12	Brazilian test	Indirect tensile strength	ASTM D3967

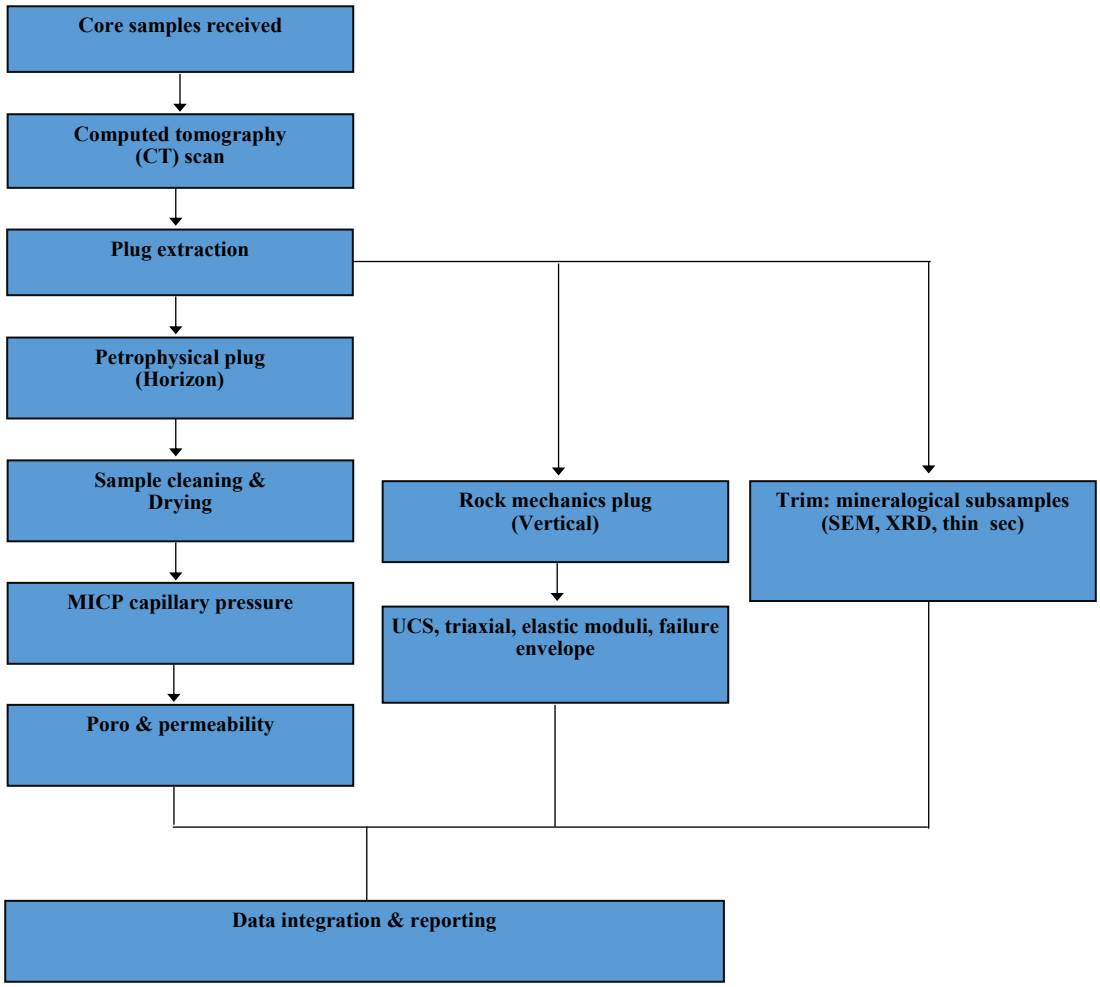

Figure 1. Workflow of core sampling, preparation, and laboratory testing for caprock integrity

Table 3. CT scan observations and core quality assessment (Well ASR-1)

Depth (ftMD)	Formation	CT Scan Observation	Core Integrity	Plug Selection Recommendation
3546	Baturaja	Homogeneous texture, minor edge disturbance	Intact	Suitable for poro–perm & UCS
3562	Baturaja	Continuous fabric, subtle bedding	Intact	Suitable for all tests
3665	Gita	Multiple oblique natural fractures	Moderately fractured	Avoid fractured zones, plugs only from intact sections
3710	Gita	Inclined fracture networks visible in axial slices	Fractured	Limited intact volume, plugs with caution
3744	Gita	Localized cracks and small voids	Moderately fractured	Extract from intact subsections only

testing, mineralogical characterization, and rock mechanics analysis. This sequence is summarized in Table 2.

Finally, all petrophysical, mineralogical, and mechanical datasets were integrated to provide a comprehensive assessment of caprock integrity. Sealing capacity was evaluated from MICP entry pressures, while mechanical stability was interpreted from UCS, triaxial test parameters, and tensile strength. Mineralogical controls on sealing and strength behavior were examined by correlating clay content and cementation fabrics (XRD and SEM observations) with porosity–permeability and capillary pressure trends. These results were then correlated with the stratigraphic depth intervals of Well ASR-1 in order to capture vertical variability and heterogeneity in caprock integrity. This integrative approach aligns with recent international practices where multiscale data integration has proven critical for robust caprock integrity assessment across different geological settings.

RESULT AND DISCUSSION

CT scan and core screening

CT scanning was performed on all core intervals to assess internal integrity, identify natural fractures, and avoid disturbed zones during plug extraction. The results are summarized in Table 3. Representative CT images are shown in Figures 2–4.

CT slices from 3546 ft (Baturaja Formation) show a largely homogeneous structure with only minor edge disturbance, indicating a high-quality interval for petrophysical and rock mechanics testing (Figure 2a). Similarly, the 3562 ft interval (Baturaja Fomation) displays continuous internal fabric with subtle layering but no major discontinuities, confirming its suitability for all types of testing (Figure 2b).

In contrast, the 3665 ft core from the Gita Formation reveals several oblique natural fractures, clearly visible in axial slices B and C (Figure 3). These fractures reduce the overall integrity of the section; however, intact regions remain available for selective plug extraction.

The 3710 ft core from the Gita Formation shows curved and inclined fracture networks, particularly evident in axial slices B and C (Figure 3). These features limit the availability of intact plug material, although localized unfractured zones remain suitable for petrophysical measurements. Finally, the 3744 ft sample (Gita Formation) presents localized cracks and isolated voids (Figure 3). Despite these heterogeneities, suitable intact sections were identified for plug preparation. Overall, CT screening demonstrated that the Baturaja Formation cores are relatively intact and homogeneous, whereas the Gita Formation exhibits more frequent natural fractures and structural heterogeneities. These differences highlight the contrasting lithological controls on caprock integrity and guided careful selection of representative plugs for subsequent laboratory testing.

Mercury injection capillary pressure (MICP)

Mercury Injection Capillary Pressure (MICP) tests were conducted on selected core plugs from Baturaja Formation to determine pore-throat size distribution, capillary sealing capacity, and threshold pressures. The results for the 3546 ft interval are shown in Figure 5.

The capillary entry pressure (Pc_entry) was measured at approximately 1,197 psi, corresponding to the minimum pressure required for a non-wetting fluid (e.g., CO_2 or mercury) to invade the smallest pore throats. The breakthrough pressure (Pc_breakthrough) was significantly higher, around 59,980 psi, representing the point at which the non-wetting phase percolates through the entire sample thickness.

The derived pore-throat diameter, calculated using the Washburn equation, was approximately 0.1325 μm, confirming a tight sealing fabric dominated by micro- to nano-sized throats. These values are consistent with typical caprock-quality intervals, suggesting that the Baturaja Formation at this depth provides an effective seal against fluid migration. Mercury injection capillary pressure (MICP) analysis was conducted on core plugs from the Baturaja and Gita formations to quantify pore-throat size distribution and capillary sealing capacity (Table 4; Figure 5).

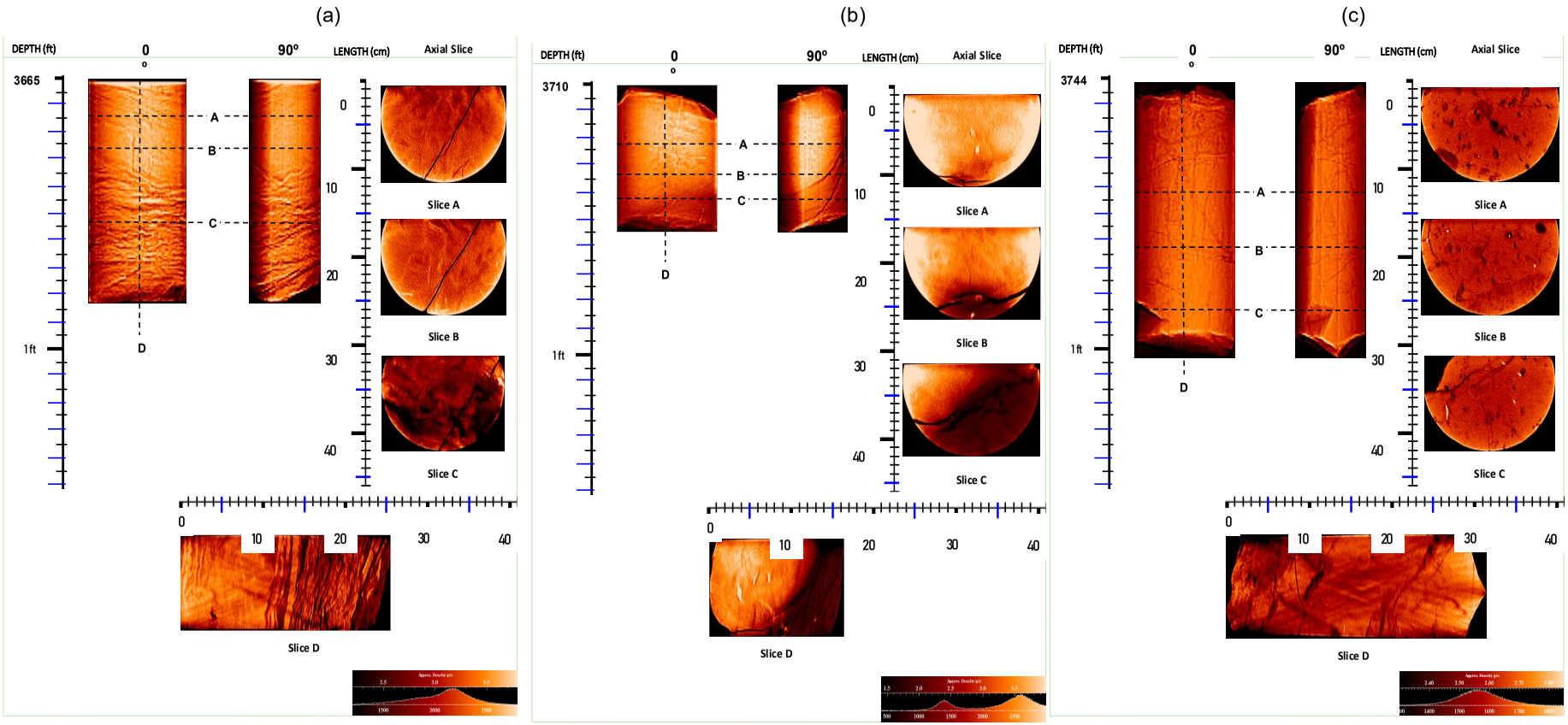

Figure 2a-2c. Representative CT images of the Baturaja formation core

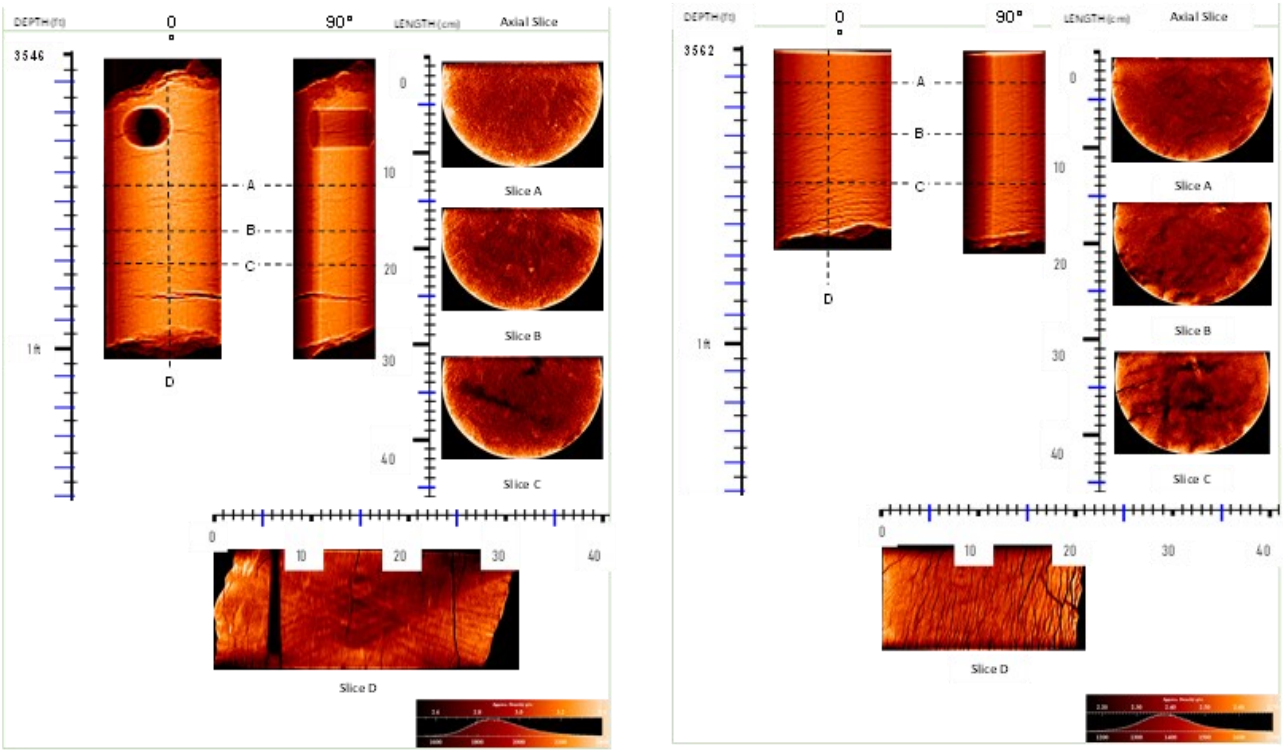

Figure 3. Natural fractures in the gita formation core

Table 4. Summary of MICP results for Baturaja and Gita Formations (Well ASR-1)

Depth (ft MD)	Formation	Pc_entry (psi)	Dominant Pore-Throat Size Class	Pore Size Distribution (%PV)	Remarks
3546	Baturaja	1,197	0.01–0.1 µm	71% (0.01–0.1 µm); 17% (0.1–1 µm)	Tight carbonate caprock with good sealing
3562	Baturaja	217	0.1–1 µm	76% (0.1–1 µm); 22% (0.01–0.1 µm)	Coarser pores, lower sealing efficiency
3665	Gita	988	<0.1 µm	92% (0.01–0.1 µm); 6% (0.1–1 µm)	Fine pores, strong sealing despite fractures
3710	Gita	2,844	0.01–0.1 µm	95% (0.01–0.1 µm)	Highest entry pressure, excellent sealing
3744	Gita	1,395	0.01–1 µm	68% (0.01–0.1 µm); 26% (0.1–1 µm)	Larger throats present, moderate sealing

The Baturaja Formation shows contrasting results between depths. At 3546 ft, the capillary entry pressure (Pc_entry) was approximately 1,197 psi, with pore volume dominated by 0.01–0.1 µm throats (71%). This tight pore network indicates a carbonate caprock with strong sealing properties. In contrast, the 3562 ft sample yielded a much lower Pc_entry of 217 psi, dominated by coarser 0.1–1 µm throats (76%), reflecting reduced sealing efficiency.

The Gita Formation generally exhibits finer pore systems and higher sealing capacity. At 3665 ft, more than 90% of pore volume was <0.1 µm, resulting in a Pc_entry of approximately 988 psi despite fractures observed in CT scans, indicating effective sealing. The 3710 ft interval showed the strongest sealing behavior, with Pc_entry of approximately 2,844 psi and 95% of pore volume in the 0.01–0.1 µm class, representing the most

robust sealing capacity of all samples tested. At 3744 ft, the pore system was more heterogeneous, with 26% of pores in the 0.1–1 µm class and Pc_entry of ~1,395 psi, indicating moderate but still effective sealing.

Overall, the MICP results demonstrate that the Baturaja Formation exhibits variable sealing capacity influenced by pore-throat size distribution, whereas the Gita Formation consistently provides strong sealing capacity, with exceptional performance at 3710 ft. These findings confirm that both formations function effectively as caprock units, albeit with lithology- dependent variability.

Seal capacity calculations were performed by converting the measured Air–Hg entry pressures to a Brine–CO_2 system, following the methodology of Daniel and Kaldi (2009, 2012) and Watts (1987). The results are summarized in Table 4.

The Baturaja Formation exhibits variable seal capacity. At 3546 ft, the Brine–CO_2 entry pressure was 68 psi, corresponding to a CO_2 column height of approximately 663 ft, while at 3562 ft, the entry pressure was only 12 psi, yielding a limited CO_2 column height of approximately 117 ft. These results reflect the contrast between the tighter pore-throat distribution at 3546 ft and the coarser pore network at 3562 ft.

The Gita Formation demonstrates generally stronger seal performance. At 3665 ft, the Brine–CO_2 entry pressure was 56 psi, supporting a CO_2 column height of approximately 547 ft. The 3710 ft interval recorded the highest seal capacity, with Brine–CO_2 entry pressure of 161 psi and the ability to sustain a CO_2 column height of ~1,570 ft, representing the most effective caprock interval in the dataset. At 3744 ft, the entry pressure was 79 psi, yielding a CO_2 column height of approximately 772 ft, still within the range of effective sealing lithologies.

Overall, these results confirm that both Baturaja and Gita Formations provide sufficient sealing capacity to retain significant CO_2 columns, with the Gita Formation at 3710 ft standing out as the strongest sealing horizon.

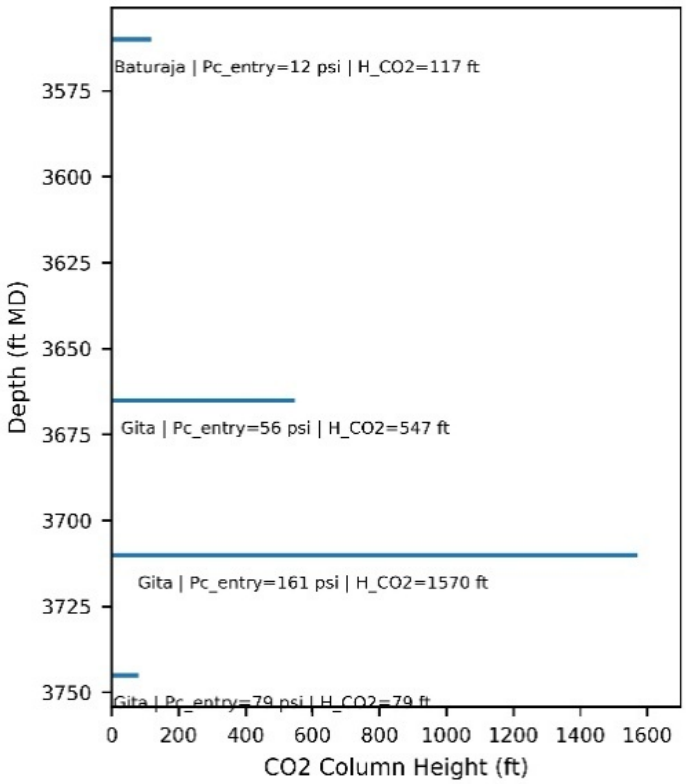

Figure 5. Estimated CO_2 column height at different depth intervals for Baturaja and Gita Formations based on capillary entry pressure (Pc_entry) and fracture pressure (Pc_break = 3400 psi). Higher Pc_entry values correspond to greater CO_2 column height capacity, indicating stronger sealing performance.

Rock mechanics analysis

Unconfined compressive strength (UCS) and triaxial compression (TCS) tests were performed on representative vertical plugs from the Baturaja and Gita formations (Table 5).

The Baturaja Formation exhibits variable mechanical properties. At 3546 ft, the sample reached a TCS of 56.7 MPa with Young's modulus of approximately 2.9 GPa and a friction angle of about 34°. Despite its adequate stiffness, cohesion was relatively low (3.8 MPa), placing this interval in a moderate stability category.

At 3562 ft, both strength and stiffness were further reduced (TCS = 40.4 MPa, E ≈ 1.6 GPa, cohesion 2.8 MPa), indicating the weakest mechanical response within the Baturaja interval.

The Gita Formation generally exhibits superior mechanical performance compared to the Baturaja intervals (Figure 6). At 3665 ft, TCS reached 100.1 MPa, accompanied by high stiffness (E ≈ 12.1 GPa; Figure 6a) and cohesion of 8.3 MPa (Figure 6b), indicating good suitability for long-term CO_2 containment.

The 3710 ft core demonstrates the highest strength (TCS = 112.5 MPa), with substantial stiffness (~10 GPa) and cohesion (16.6 MPa), representing the most mechanically robust sealing unit. This mechanical robustness aligns with the highest MICP entry pressure (2,844 psi; Figure 6c). Although the friction angle (~45°) is favorable, this interval is mechanically sensitive under elevated pore pressures and is therefore categorized as moderately stable. Overall, the Gita Formation provides superior mechanical sealing capacity compared to Baturaja Formation. The strongest sealing performance occurs at 3710 ft, where high UCS, stiffness, and cohesion coincide with excellent petrophysical sealing from MICP results. In contrast, the Baturaja 3562 ft sample represents a weaker interval that may require careful monitoring of injection pressures.

These findings confirm that caprock integrity is depth- and lithology-dependent, with mechanical robustness broadly aligning with pore-throat distributions observed in MICP tests.

Integrated thin-section petrography, sem, and XRD analyses

Thin-section petrography, SEM-EDX, and XRD analyses provide detailed mineralogical and textural characterization of the caprock intervals.

At 3546 ft, the volcanic sandstone (litharenite) contains illite (10.5%), smectite (4.9%), kaolinite (1.7%), and significant calcite cement (46.8%). Visual porosity is low (4.25%), dominated by secondary dissolution pores. SEM observations indicate illite and dolomite cementation, with microporosity present within clay minerals and fossils fragments.

The 3562 ft sandy dolostone is strongly dominated by dolomite (71.1 wt%) with minor illite (7.0%) and quartz (17.6%). Porosity is very

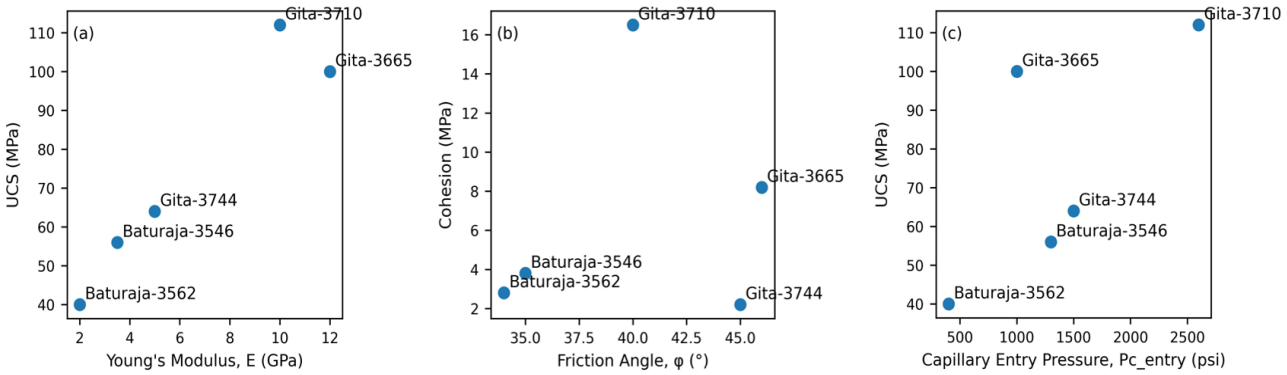

Figure 6. (a) Relationship between Young's Modulus (E) and UCS showing that Gita Formation exhibits higher stiffness and strength compared to Baturaja intervals. (b) Cohesion–friction angle distribution illustrating mechanical heterogeneity; the 3710 ft interval shows significantly higher cohesion. (c) Positive correlation between capillary entry pressure (Pc_entry) and UCS, indicating that mechanically stronger intervals tend to exhibit better sealing capacity.

Table 5. Thin-section petrography, SEM & XRD Results

Depth (ft)	Dominant Mineralogy	Porosity	Main Microstructural Features
3546	Calcite-dominated carbonate with illite–smectite clays	Very low (~4.25%)	Microporosity in clays and fossils, minor dissolution pores
3562	Dolomite-dominated carbonate with quartz and clays	Very low	Intercrystalline dolomite micropores and minor dissolution pores
3665	Calcite–dolomite carbonate with minor siderite	Very low (~1.0%)	Secondary dissolution pores and carbonate cementation
3710	Siderite-dominated interval with minor quartz and clays	Very low	Microporosity in siderite matrix, possible microfractures
3744	Quartz-dominated interval with minor clays	Very low (~0.75%)	Quartz overgrowths and micropores in clay minerals

low, mostly intercrystalline, with dolomite cement observed under SEM. Diagenesis is characterized by dolomite replacement and minor dissolution.

At 3665 ft, limestone samples are dominated by calcite (73.3 wt%) and dolomite (20.3%), with very low visual porosity (1.0%). SEM images show calcite–dolomite cementation with secondary dissolution pores. The rock texture is floatstone, dominated by carbonate mud and skeletal grains.

The 3710 ft sideritic claystone is overwhelmingly siderite-rich (85.2 wt%), with small amounts of illite (3.0%) and kaolinite (3.7%). Porosity is extremely low and primarily associated with siderite-rich matrices. SEM-EDX observations indicate siderite alteration with minor microporosity, while diagenesis is dominated by siderite replacement.

Finally, at 3744 ft, the quartzarenite is almost pure quartz (95.9 wt%), with accessory kaolinite (2.0%) and illite (1.9%). Porosity is 0.75%, mainly consisting of secondary dissolution pores. SEM observations show quartz overgrowths and microporosity within clay minerals.

Overall, the mineralogical and petrographic data confirm significant heterogeneity between formations. Quartz-dominated sandstone (3744 ft) provides strong mechanical integrity, carbonate-rich intervals (3562–3665 ft) exhibit geochemical reactivity with CO_2, while sideritic claystone (3710 ft) has strong sealing potential due to siderite cementation and extremely low porosity.

Discussion – integrated caprock integrity assessment

The integration of petrophysical (MICP), mechanical, and mineralogical results provides a comprehensive evaluation of caprock integrity in Well ASR-1.

MICP analysis indicates significant variation in sealing capacity between intervals. The Baturaja samples (e.g., 3562 ft) exhibit relatively low entry pressures (Pc_entry = 12 psi) and limited CO_2 column heights (~117 ft), reflecting coarser pore-throat distributions. In contrast, the Gita formation (e.g., 3710 ft) demonstrates the highest entry pressure (Pc_entry = 161 psi) and CO_2 column height (~1570 ft), confirming its superior sealing capacity.

Mechanical testing supports these findings. The Gita formation shows the highest UCS (100–112 MPa) and Young's modulus (>9 GPa), consistent with strong mechanical resistance to failure under injection pressures. The Baturaja intervals, while competent, exhibit moderate UCS values (40–57 MPa) and lower elastic moduli, implying greater susceptibility to shear failure.

Cohesion and friction angle values further highlight the mechanical robustness of the Gita Formation compared to the more carbonate-rich Baturaja intervals.

Mineralogical evidence explains these trends. Quartz dominates the Gita formation (>95%), imparting strong mechanical integrity with minimal

geochemical reactivity. In contrast, Baturaja samples contain higher proportions of carbonates (calcite and dolomite up to 71%), which, while mechanically weaker, offer potential for geochemical trapping of CO_2 through mineralization reactions.

The sideritic claystone at 3710 ft is particularly notable, combining high siderite content (85%) with strong sealing properties due to siderite cementation and extremely low porosity.

Taken together, these results suggest a dual sealing mechanism: (i) mechanical–capillary sealing, dominated by quartz-rich and siderite- rich lithologies (Gita Formation, 3710–3744 ft), and (ii) geochemical sealing, contributed by carbonate-rich intervals within the Baturaja Formation. This multi -barrier sealing system enhances the long-term security of CO_2 storage by providing both physical and chemical containment mechanisms.

CONCLUSION

This study integrated CT scanning, MICP analysis, rock mechanics testing, and mineralogical characterization to evaluate the caprock integrity of the Baturaja and Gita Formations in Well ASR-1. The main findings are as follows:

- Capillary sealing capacity

MICP results reveal strong vertical variability. The Gita Formation, particularly at 3710 ft, exhibits the highest entry pressure (161 psi) and CO_2 column height (>1500 ft), indicating excellent sealing capacity. In contrast, the Baturaja samples show weaker sealing performance with lower Pc_entry values.

- Mechanical Integrity

Rock mechanics testing confirms that quartz-rich and siderite- rich intervals possess superior mechanical properties (UCS >100 MPa, E >9 GPa), whereas carbonate-rich intervals exhibit lower strength and stiffness but still retain moderate sealing potential.

- Mineralogical controls

XRD and SEM analyses reveal that quartz dominance in the Gita formation enhances mechanical stability, while carbonate-rich intervals in the Baturaja Formation provide additional geochemical trapping potential. The sideritic claystone at 3710 ft combines both mechanical sealing and mineral trapping capacity.

- Integrated multi-mechanism system

Integrated Multi-Mechanism System – Stratigraphic integration highlights a stacked sealing system, where quartz provides mechanical barriers, carbonates enhance geochemical reactivity, and siderite contributes mineral trapping. This multi-barrier framework ensures long-term storage security under CO_2 injection scenarios.

These findings demonstrate that reliable CO_2 storage requires not only mechanical and petrophysical assessments but also mineralogical characterization. The Gita formation represents the most effective sealing interval, while Baturaja carbonates may complement storage security through geochemical reactions. Integrating laboratory workflows with stratigraphic analysis provides a robust approach for site selection, risk assessment, and caprock qualification in CCS projects.

ACKNOWLEDGEMENT

This research was conducted through collaborative experimental and analytical activities carried out at several institutions, including the Energy Building (7th Floor), Enhanced Oil Recovery (EOR) Laboratory, Faculty of Mining and Petroleum Engineering, Bandung Institute of Technology (ITB), Jalan Ganesha No. 10, Bandung; the Petroleum Engineering Laboratory, Universitas Pembangunan Nasional “Veteran” Yogyakarta; and the laboratory facilities of Universiti Malaya, Kuala Lumpur, Malaysia. The study was fully supported by institutional research funding provided by LPPM Universitas Pembangunan Nasional “Veteran” Yogyakarta under Grant No. 444/UN62.21/PG.00.00/2025.

GLOSSARY OF TERM OF SYMBOLS

Terms & Symbols	Definition	Unit
ASTM	American society for testing and materials	–
AFR	Air-to-fuel ratio	kg air/kg fuel
EMR	Energy and mineral resources	–
CH_4	Methane	–
SiO_2	Silica	–
k_a	Absolute permeability	millidarcy (mD)
w	Weight	gram (g)
α	Angle of internal friction	degree (°)
ρ_β	Bulk density	g/cm³
Pc_entry	Capillary entry pressure (minimum pressure for non-wetting phase invasion)	psi
MICP	Mercury injection capillary pressure	–
UCS	Unconfined compressive strength	MPa
E	Young's modulus	GPa
ν	Poisson's ratio	–
CT	Computed tomography	–
XRD	X-ray Diffraction	–
SEM–EDS	Scanning Electron Microscopy with Energy-Dispersive Spectroscopy	–

REFERENCES

Ajayi, T., J. S. Gomes, & A. Bera. (2019), A Review of CO_2 Storage in Geological Formations Emphasizing Modeling, Monitoring and Safety. Petroleum Science and Technology. doi:10.1007/s12182-019-0340-8.

Ali, M., (2021), Influence of Pressure, Temperature and Organic Surface Concentration on Hydrogen Wettability of Caprock; Implications for Hydrogen Geo-Storage. Energy Reports 7:5988–96. doi:10.1016/j.egyr.2021.09.016.

Al-Yaseri, Ahmed, Abduljamiu Amao, & Ahmed Fatah, (2023), Experimental Investigation of Shale/Hydrogen Geochemical Interactions." Fuel 346:128272. doi:10.1016/j.fuel.2023.128272.

Ao, Xiang, Yiyu Lu, Jiren Tang, Yuting Chen, & Honglian Li, (2017), Investigation on the Physics Structure and Chemical Properties of the Shale Treated by Supercritical CO_2. Journal of CO_2 Utilization 20:274–81. doi:10.1016/j.jcou.2017.05.028.

Bera, A., B. Shukla, & D. Jogani, (2025), A Perspective Review of Applications of the Computed Tomography (CT) Scan Imaging Technique for Microscopic Reservoir Rock Characterization. Deep Underground Science and Engineering. doi:10.1002/dug2.12138.

Boulin, P. F., P. Bretonnier, & V. Vassil, (2013), Seal Capacity: Influence of Stress and Geometry on Capillary Entry Pressure. Marine and Petroleum Geology 48:64–73. doi:10.1016/j.marpetgeo.2013.07.010.

Bourbiaux, B.,(2007), Multi-Scale Characterization of an Heterogeneous Aquifer Through the Integration of Geological, Geophysical and Flow Data: A Case Study." Oil & Gas Science and Technology 62(3):347–73. doi:10.2516/ogst.

Busch, A., S. Alles, Y. Gensterblum, D. Prinz, D. N. Dewhurst, M. D. Raven, H. Stanjek, & B. M. Krooss, (2008). Carbon Dioxide Storage Potential of Shales. International Journal of Greenhouse Gas Control 2(3):297–308. doi:10.1016/j.ijggc.2008.03.003.

Chiquet, P., J. L. Daridon, D. Broseta, & S. Thibeau, (2007), Wettability Alteration of Caprock Minerals by Carbon Dioxide. Geofluids 7(2):112–22. doi:10.1111/j.1468-8123.2007.00168.x.

Choi, C. S., J. Kim, & J. J. Song, (2021), Analysis of Shale Property Changes after Geochemical Interaction under CO2 Sequestration Conditions. Energy 214:118933. doi:10.1016/j.energy.2020.118933.

Destiana, Syifa, Dedy Irawan, Prasandi Abdul Aziz, & Ika Merdekawati, 2025. CO_2 Storage Screening Criteria Based on Seal Capacity in Indonesia. Scientific Contributions Oil and Gas 48(4). https://doi.org/10.29017/scog.v48i4.1829

Farokhpoor, R., B. J. A. Bjørkvik, E. Lindeberg, & O. Torsæter, (2013), Wettability Behaviour of CO_2 at Storage Conditions." International Journal of Greenhouse Gas Control 12:18–25. doi:10.1016/j.ijggc.2012.11.003.

Fisher, Q. J., M. Casey, S. D. Harris, and R. J. Knipe, (2001), Uncertainty in Fault Seal Parameters: Implications for Hydrocarbon Retention." Marine and Petroleum Geology 18 (4):469–88. doi:10.1016/S0264-8172(00)00064-7.

Hansen, O. R., (2020), Caprock Integrity Assessment from MICP, Pore Pressure and Geomechanical Constraints. Marine and Petroleum Geology 121:104603. doi:10.1016/j.marpetgeo.2020.104603.

Kadyrov, R., E. Statsenko, & T. H. Nguyen, (2024), Integrating MCT Imaging of Core Plugs and Transfer Learning for Automated Reservoir Rock Characterization and Tomofacies Identification." Marine and Petroleum Geology 165:107014. doi:10.1016/j.marpetgeo.2024.107014.

Klewiah, I., D. S. Berawala, H. C. A. Walker, P. Ø. Andersen, & P. H. Nadeau, (2020), Review of Experimental Sorption Studies of CO_2 and CH4 in Shales." Journal of Natural Gas Science and Engineering 74:103045. doi:10.1016/j.jngse.2019.103045.

Liang, Z., (2022), Study and Classification of Porosity Stress Sensitivity in Shale." ACS Omega 7(31):27377–90. doi:10.1021/acsomega.2c03393.

Lin, R., (2022), Stress and Pressure Dependent Permeability of Shale Rock: Discrete Element Method (DEM) Simulation on Digital Core. Journal of Petroleum Science and Engineering 208:109797. doi:10.1016/j.petrol.2021.109797.

Lohr, C. D., & P. C. Hackley, (2018), Using Mercury Injection Pressure Analyses to Estimate Sealing Capacity of the Tuscaloosa Marine Shale in Mississippi, USA: Implications for Carbon Dioxide Sequestration." International Journal of Greenhouse Gas Control 75:186–99. doi:10.1016/j.ijggc.2018.09.006.

Miocic, J. M., G. Johnson, & C. E. Bond, (2019), Uncertainty in Fault Seal Parameters: Implications for CO_2 Column Height Retention and Storage Capacity in Geological CO_2 Storage Projects. Solid Earth 10(3):951–67. doi:10.5194/se-10-951-2019.

Mouzakis, Katherine M., Alexis K. Navarre-Sitchler, Gernot Rother, José Leobardo Bañuelos, Xiuyu Wang, John P. Kaszuba, Jason E. Heath, Quin R. S. Miller, Vladimir Alvarado, and John E. McCray, (2016), Experimental Study of Porosity Changes in Shale Caprocks Exposed to CO_2-Saturated Brines I: Evolution of Mineralogy, Pore Connectivity, Pore Size Distribution, and Surface Area." Environmental Engineering Science 33(10):725–35. doi:10.1089/ees.2015.0588.

Nugraha, Fanata Y., M. Firdaus Al Hakim, Brian Tony, Damar Nandiwardhana, & Steven Chandra, (2024), Development of CO_2 Hub-Clustering Management in The South Sumatra Basin. Scientific Contributions Oil and Gas 47 (1). https://doi.org/10.29017/SCOG.47.1.1607.

Olabode, A., & M. Radonjic, (2014) "Characterization of Shale Cap-Rock Nano-Pores in Geologic CO_2 Containment." Environmental & Engineering Geoscience 20 (4):361–70. doi:10.2113/gseegeosci.20.4.361.

Paulsen, S. 2022. "Quantifying Caprock Integrity under CO2 Injection: Integrating Geomechanics and Petrophysics." Marine and Petroleum Geology 143:105588. doi:10.1016/j.marpetgeo.2022.105588.

Purba, Humbang, Bagus D. Prasetyo, Ricky Andrian Tampubolon, Pradityo Riyadi, Shidqi Anugrah Diria, & Argya H. Basundara, (2017), "Pemisahan Litologi dan Fluida Dengan Menggunakan Poisson Impedance (Distinguishing Lithology and Fluid Using Poisson Impedance)." Lembaran Publikasi

Minyak dan Gas Bumi 51(3). https://doi.org/10.29017/LPMGB.51.3.25.

Skerbisch, A. 2025. Caprock Integrity Assessment for CO2 Storage: Core-Scale Workflow Integrating XRD, SEM-EDS, CT and MICP. International Journal of Greenhouse Gas Control 138:104434. doi:10.1016/j.ijggc.2025.104434.

Zou, Y., (2018), Effects of CO_2–Brine–Rock Interaction on Porosity/Permeability and Mechanical Properties during Supercritical-CO_2 Fracturing in Shale Reservoirs." Journal of Natural Gas Science and Engineering 53:102–15. doi:10.1016/j.jngse.2017.11.004.